Comparison of Sea Surface Dynamic Heights Estimated from Inverted Echo Sounder Data and Satellite Altimeter Data

Koji KAKINOKI[*1,†] Shiro IMAWAKI[*1,2]
Kaoru ICHIKAWA[*1,2,3] and Shin-ichiro UMATANI[*1,2]
[†]E-mail of corresponding author: *kakinoki@riam.kyushu-u.ac.jp*

Sea surface dynamic height (SSDH) anomalies estimated from long-time inverted echo sounder (IES) data using gravest empirical mode method are compared with satellite altimeter data. The IES-derived SSDH anomalies agree well with the altimetric SSDH anomalies, although the IES-derived SSDH variation is slightly underestimated. We calculate power spectra of these SSDH anomalies to discuss time-scale dependency of their differences. The differences between two SSDH anomalies are found mainly caused by components with the periods from 50 days to 100 days, which correspond to meso-scale eddies or small meanders of the Kuroshio. These differences result in smaller variation of the IES-derived SSDH.

Key words: *sea surface dynamic height, inverted echo sounder, satellite altimeter, Kuroshio*

1. Introduction

Inverted echo sounders (IESs) set on the sea floor repeatedly measure the round-trip acoustic travel time between the sea floor and sea surface. As the travel time is a depth integral of the inverse of the sound speed[1], travel time variations reflect the depth variations of the main thermocline well since temperature strongly influence sound speed.

A method called the gravest empirical mode (GEM) has been developed[2], which estimates the vertical profiles of the temperature and the density from the IES data. The method has been applied in the Kuroshio region south of Japan[3,4]. Book *et al.* (2002)[3] clearly demonstrated that the temperature and specific-volume-anomaly estimated from the GEM fields describe the hydrographic data very well. Kakinoki *et al.* (2006, hearafter KE06)[4] has been obtained a long time series of sea surface dynamic heights (SSDHs) from a long time series of travel time combining some IES data. KE06[4] compared the IES-derived SSDHs with hydrographic SSDHs but could not discuss on the difference between two SSDHs. The purpose of this paper, therefore, is to compare SSDH anomalies estimated from long-time IES data with SSDH anomalies estimated from satellite altimeter data and to discuss on their differences, accounting their time scale dependency. First, data used in this study are described in Section 2. Next, we statistically compare the IES-derived SSDH anomalies with the altimetric SSDH anomalies (Section 3). In addition, we calculate the power spectra of these SSDH anomalies to discuss time-scale dependency of their differences (Section 4). Finally, results are summarized in Section 5.

2. Data

The IES data used in this study are obtained during October 1993 to July 2004 at coastal site ES01 (32.6°N, 133.2°E) and offshore site ES07 (31.0°N, 134.1°E) on the ASUKA line (Fig. 1). Eight tidal constituents (K1, O1, P1, Q1, M2, S2, N2, and K2) were removed from travel time data by the harmonic analysis. The travel time data were low-pass filtered using a Butterworth filter with a 50-hour cut-off period and were resampled four times a day[5]. In addition, the data were low-pass filtered using a box filter with a 9-day cut-off period. The details of the IES data are described in

*1　Research Institute for Applied Mechanics
*2　Department of Earth System Science and Technology
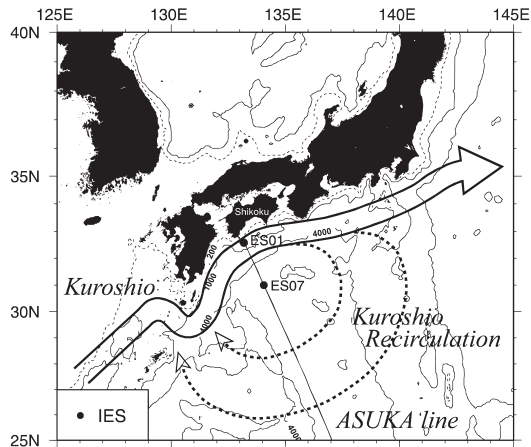*3　Japan Agency for Marine-Earth Science and Technology

Fig.1 Locations of the IES observations on the ASUKA line. Dots indicate the coastal station (ES01) and offshore station (ES07) across the Kuroshio where the IES observations were maintained after the ASUKA intensive survey. Thick line shows the schematic flow patterns of the Kuroshio. Dashed thick line shows the Kuroshio recirculation. Water depth is indicated by a dashed line (200 m) and a narrow solid line (1000 m and 4000 m).

KE06[4]. The IES-derived SSDHs were subsampled at the observational times of the altimetry data; we calculated anomalies from the sample average of the IES-derived SSDHs.

A set of hydrographic data near the ES01 and ES07 is used, which were obtained using conductivity-temperature-depth recorder (CTD) and expendable bathy-thermograph (XBT) data from November 1992 to September 2002. Because XBT cannot observe salinity, the salinity for XBT data is estimated from the temperature-salinity (T-S) relationship in the Kuroshio region off Shikoku calculated from the CTD data on the ASUKA line;

the T-S relationships were separately determined for the coastal and offshore sites.

The SSDH anomalies observed by TOPEX/POSEIDON (T/P) and Jason-1 were used to be compared with the IES-derived SSDHs. The altimetric products were provided by the Goddard Space Flight Center of National Aeronautics and Space Administration (T/P data) and Ssalto (Jason-1 data)[6]. The T/P data are colinear sea surface heights data. Jason-1 data are the delayed-time updated sea level anomalies. The observation intervals are 9.92 days. We used the SSDH anomaly data at the closest points to the IES sites.

We use the SSDH data estimated from IES data in KE06[4]. To construct a GEM field that is applicable throughout a year, KE06[4] removed seasonal variation in surface layer where the surface layer is defined as the layer between the sea surface and 150 dbar. KE06[4] obtained seasonal variation components of temperature as an annual sinusoidal function by applying the harmonic analysis to hydrographic data in the surface layer, and also estimated seasonal components of the travel time of the surface layer and the SSDH referred to 150 dbar from the hydrographic data. This temporal variation is used to remove the hydrographic SSDH referred to 150 dbar from the altimeter data.

3. Comparison with Altimetry Data

The altimetric SSDH anomaly includes the baroclinic and barotropic components, but the hydrographic and the IES-derived SSDHs only include the baroclinic component. We examine at which depth almost baroclinic signal can be extracted (Table 1). We estimated the hy-

Table 1 Summary of the comparisons of the SSDH anomalies. Reference level indicates the pressure level used to calculate the SSDH anomalies. Left side of the pair for the comparisons is the abscissa.

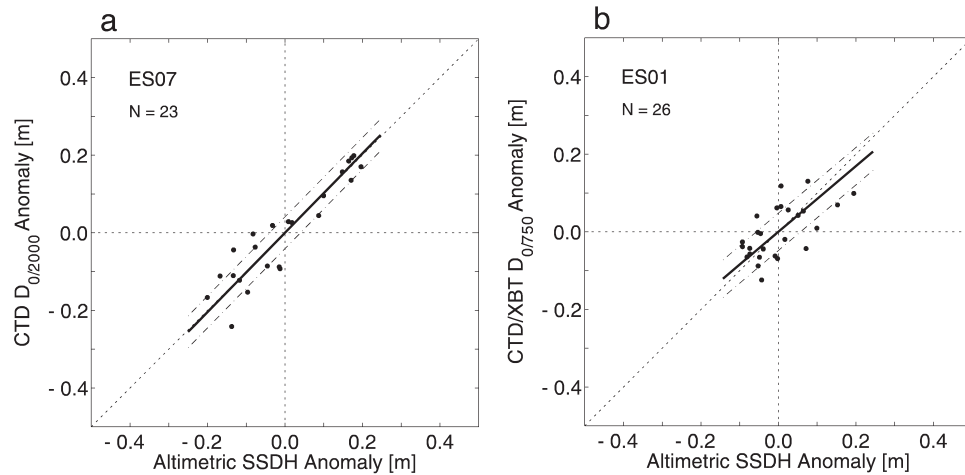| Station	Pair	Correlation coefficient	Slope	RMS (cm)	N	Reference level (dbar)
ES01	CTD/XBT vs. Altimeter	0.61	0.85	3.7	26	750
	Altimeter vs. IES	0.57	0.80	4.0	198	750
ES07	CTD vs. Altimeter	0.92	0.78	2.4	23	1000
		0.92	0.94	2.7	23	1500
		0.92	1.02	2.9	23	2000
		0.90	1.00	3.0	23	2500
	Altimeter vs. IES	0.89	0.80	3.6	276	2000

Fig.2 Scatter plots of the SSDH anomalies obtained by hydrography and altimetry. Original hydrographic SSDH anomaly is abscissa. Solid line shows the regression line. Chain line indicates the rms difference from the regression line. Dotted line shows the one-to-one line. (a) Stn. ES07. Reference level is 2000 dbar. (b) Stn. ES01. Reference level is 750 dbar.
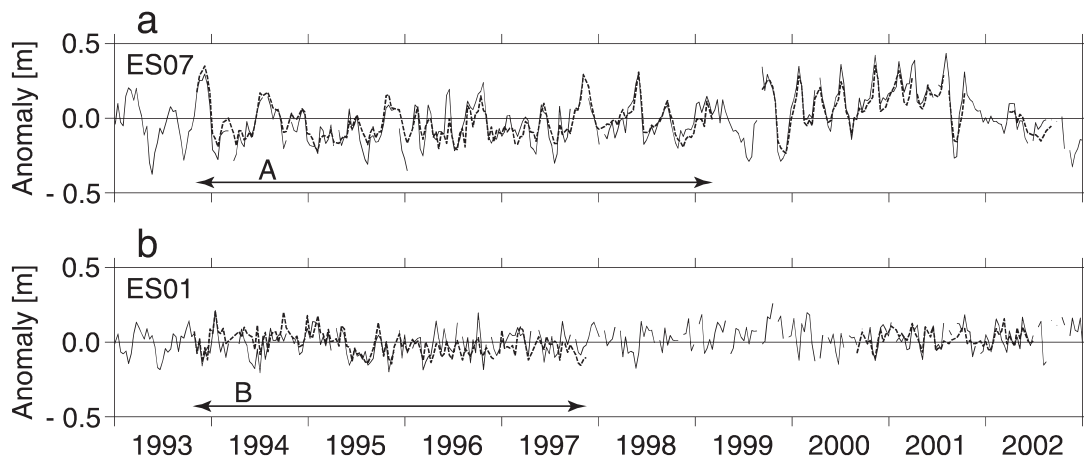

Fig.3 Time series of the SSDH anomalies obtained by IES and altimetry. Dashed lines illustrate the IES data. Solid line shows altimetry data. A and B show the each study period in which the power spectrum is calculated. (a) Stn. ES07. Reference level is 2000 dbar. (b) Stn. ES01. Reference level is 750 dbar.

drographic SSDHs referred to 1000, 1500, 2000, and 2500 dbar. The altimetric SSDH anomalies were interpolated at the observational times of the hydrographic data; we calculated anomalies from the sample average. The variations of the altimetric SSDH anomalies agreed well with those of the hydrographic SSDH anomalies referred to deeper 2000 dbar since slope of the regression line is close to the unity (Fig. 2(a)). For the coastal site, we estimated the hydrographic SSDHs referred to 750 dbar near the sea bottom. The variations of the altimetric SSDH anomalies agreed with those of the hydrographic SSDH anomalies referred to 750 dbar (Fig. 2(b)).

The IES-derived SSDHs are compared to the altimetric SSDH anomalies. In Fig. 3, the IES-derived SSDH anomaly variation for the offshore site describes the altimetric SSDH anomaly variation very well, although the amplitude of the former is slightly small, which seems to be caused by using GEM method. Table 1 shows the statistical results. For the offshore site, the correlation coefficient is higher and the root-mean-square (rms) difference from the regression line is smaller than those for the coastal site, and slope of the regression line is 0.80.

4. Time Scale Dependency of Sea Surface Dynamic Height Error

Although we statistically compared the IES-derived SSDH with the altimetric SSDH anomaly in the previous section, we have not yet identified the sources of their discrepancies.

Therefore in this section, we calculate the power spectra of these SSDH anomalies to discuss time-scale dependency of their differences.

We select the continuous IES observations as study periods (Fig. 3); from November 1993 to November 1997 at the coastal site and from November 1993 to March 1999 at the offshore site. Missing values during each study period are linearly interpolated. The IES data are subsampled at every 10 days to match up with the altimeter data. It should be noted, however, that the IES data have been low-pass-filtered to exclude high-frequency noises. Meanwhile, the altimeter data includes noises which may cause pseudo energy density in the high-frequency domain. All power spectra are smoothed using 5-point running mean in the frequency domain. In addition, we calculate the squared coherency in order to examine the phase difference between each instrument, and periods are masked in Fig. 4 for which squared coherency between the IES and the satellite altimeter is less than 90% confidence level.

Figure 4(a) shows the power spectra at the offshore site. The squared coherency between the IES and the satellite altimeter as a whole is high, but is small for periods under 50 days; we consider this is caused by noises in the altimeter data. Energy density of the IES basically tends to be the same as that of the altimeter data for periods over 50 days, although it is slightly smaller than that of the altimeter for periods from 35 days to 230 days. Especially, a heap of the altimetry energy density for periods from 55 days to 80 days is significantly different. These periods correspond to time scale of meso-scale eddies. One of the reasons for the significantly different is the difference of density field between the Kuroshio and the meso-scale eddies. Density field variation caused by presence of such a meso-scale eddy is generally different from that caused by variation of the Kuroshio itself, but the GEM method used for the IES data cannot distinguish them as far as their travel time is the same. If the number of observations measuring meso-scale eddies is smaller than that measuring variation of the Kuroshio, the determined GEM field tends to be biased to the density field caused by variation of the Kuroshio, and thus density field under presence of a meso-scale eddy is not well represented. However, the differences of the energy densities are too large. Other reason is the difference of the vertical structures between the Kuroshio and the meso-scale eddies.
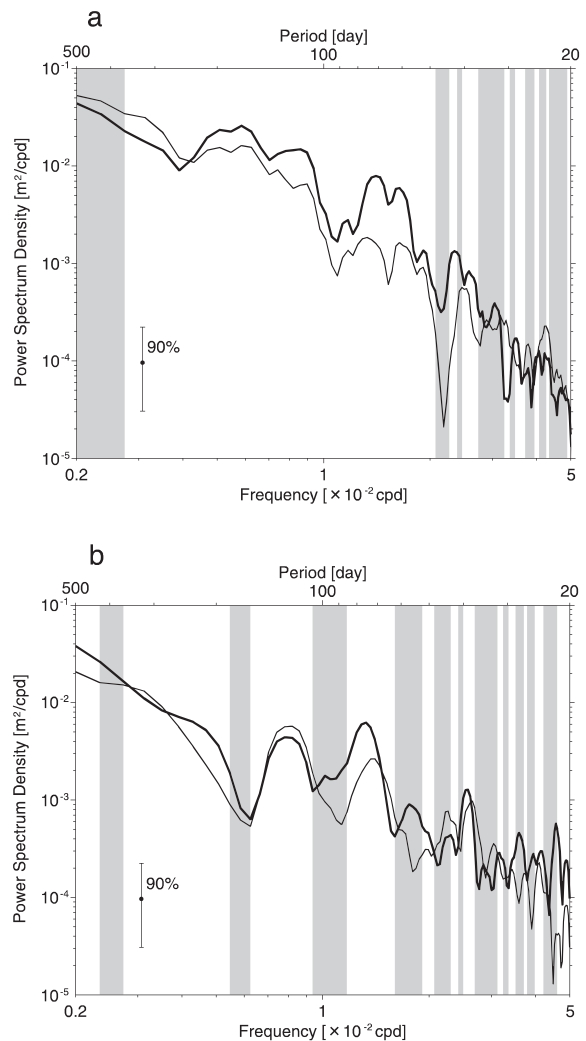

Fig.4 Power spectra of SSDHs. Solid lines show the IES spectra. Thick lines indicate the altimetric spectra. Time interval is 10 days. Error bars show the 90% confidence level. Shaded areas illustrate less than 90% confidence level of squared coherency of the IES-derived SSDH and the altimetric SSDH anomaly. (a) November 1993 to March 1999 at Stn. ES07. (b) November 1993 to November 1997 at Stn. ES01.

For the Kuroshio, pressure of no motion is approximately 2000 dbar (Fig. 2(a)), but may be deeper for the occasional meso-scale eddies. We need to compare the hydrographic SSDH anomalies with the altimetric SSDH anomalies as seen Fig. 2(a) using the hydrographic data and altimeter data which observe meso-scale eddies. These would explain the small slope of the regression line in Section 3.

Figure 4(b) shows the power spectra at the coastal site. The squared coherency between the IES and the satellite altimeter as a whole is smaller than that of the offshore site; periods exceeding the 90% confidence level are from 65 days to 85 days, from 110 days to 150 days and from 180 days to 365 days. Lower

squared coherency under 50-day period is similar to that at the offshore site, but the low squared coherency is also found around 100 days or 180 days. Although details are uncertain, one possible explanation is due to the higher mode of seasonal variation; since response of the steric height in coastal areas are generally rapid to changes of heat fluxes, distortion of the steric height from simple sinusoidal curve used in this study would be large, which results in the higher modes. Among the periods with larger coherency, energy density of the satellite altimeter is larger than that of the IES around 80 days. This discrepancy around 80 days is also considered to be meso-scale eddies.

Note that there are heaps of the energy density around 40 day both for the coastal site and the offshore site. Although the squared coherency is small, this small squared coherency would be due to the low frequency resolution of the satellite altimeter, so that the heap of the IES data may be significant. Actually, if we calculate the power spectra of the IES-derived SSDH which has 6-hour interval (figures are not shown here), significant presence of the heap is confirmed with a peak at 38 day both for the coastal site and the offshore site: the detailed description of this variation would be summarized in another document.

5. Summary

The IES-derived SSDH anomalies agree well with the altimetric SSDH anomalies at the offshore site, although the IES-derived SSDH variation is slightly underestimated. The differences between the IES-derived SSDH anomalies and the altimetric SSDH anomalies are found from the periods from 50 days to 100 days which correspond to meso-scale eddies or small meanders of the Kuroshio. These differences result in smaller variation of the IES-derived SSDH.

References

1) T. Rossby et al., J. Geophys. Res., 74, 5542–5546 (1969).
2) C. S. Meinen et al., J. Geophys. Res., 105(C9), 21,869–21,891 (2000).
3) J. Book et al., J. Geophys. Res., 107(C9), 3121 (2002), doi: 10.1029/2001JC000795.
4) K. Kakinoki et al., Bull. Res. Inst. for Applied Mechanics, Kyushu Iniv., 130, 11-20 (2002).
5) E. Fields et al., Tech. Rep. 91-3, Grad. Sch. of Oceanogr., Univ. of R.I., U.S.A.
6) AVISO, "SSALTO/DUACS user handbook", SALP-MU-P-EA-21065-CLS (2004), p.228.